

Selection of dormant cells during treatment of T-lineage lymphoblastic leukemia and CREB as a therapeutic target

The slower clearance of acute lymphoblastic leukemia (ALL) cells during induction therapy is associated with an increased risk of relapse. Insight into the mechanism(s) of the multidrug resistance, which these cells clearly display, may lead to more specific, minimal residual disease (MRD)-directed therapies. We have recently reported on the use of single-cell, high dimensional mass cytometry to functionally characterize B-lineage ALL cells in both drug-naïve cells at disease presentation and in those persisting during induction.¹ The large panel of more than 30 antibodies allowed for the discrimination of leukemia cells from normal cells, based on the identification of a leukemia-associated immunophenotype (LAIP), and provided information on cell cycle, apoptosis and the activation state of key signaling pathways, known to be recurrently activated in ALL. We demonstrated the presence of a strongly activated CREB pathway across a broad spectrum of cytogenetic groups and, using high dimensional anal-

yses, showed that activated CREB was prominent in all viable cell clusters at both presentation and in MRD. We also showed that minor subpopulations with hyperactive CREB visible at presentation had a selective advantage during induction therapy. Furthermore, using a specific inhibitor of CREB transcriptional function, we validated CREB as a therapeutic target in ALL cells. Here, we expand on our previous study using a mass cytometric antibody panel specific for T-lineage ALL (T-ALL) and similarly show the presence of activated CREB in almost all viable cell clusters during therapy, their sensitivity to CREB inhibition and importantly show that MRD is made up of non-cycling cells that appear to be selected for during therapy. These data suggest that MRD-directed therapies should be cell cycle-independent and that the CREB pathway is a valid therapeutic target in T-ALL and, as we have previously shown, B-lineage ALL.

Bone marrow samples were accessed through the New-

Table 1. Details of patients used in the study.

Sample ID	Sex	Flow MRD ALL %	ALL cell numbers analyzed by CyTOF	Age in years at presentation	Presentation WBC x10 ⁹ /L	Survival status
LK970 Presentation	Male	74.95	209,263	11	316	Alive
LK14 Presentation	Female	86.7	69,828	11	450	Alive
LK134 Presentation	UN	77.9	46,967	UN	UN	UN
LK145 Presentation	Male	2.26*	2,239	2	50	Alive
LK189 Presentation	Male	74.98	78,564	18	92	Alive
LK203 Presentation	Male	76.81	54,573	4	760	Alive
LK214 Presentation	Male	64.9	50,094	11	43	Alive
LK214 MRD day 8		12.95	14,318			
LK223 Presentation	Female	90	118,289	4	294	Alive
LK223 MRD day 8		15.6	565			
LK223 MRD day 29		0.3	104			
LK287 Presentation	Male	69.69	111,012	15	183	Alive
LK287 MRD day 21		37.03	22,883			
LK287 MRD day 29		4	821			
LK290 Presentation	Male	89.95	68,762	16	76	Alive
LK296 Presentation	Male	95.72	74,729	13	20	Alive
LK304 Presentation	Male	5.60**	98,906	5	11	Alive
LK342 Presentation	Male	80.1	105,999	8	91	Alive
LK342 MRD day 29		Positive by PCR**	189			
LK350 Presentation	Male	80.54	103,067	1	578	Died from disease
LK350 MRD day 8		56.7	171,494			
LK350 MRD day 29		13.33	11,810			

Minimal residual disease (MRD) was assessed using flow cytometry following the principles of our standardized method for B-lineage acute lymphoblastic leukemia (ALL) and involved 5 panels of 6 antibody combinations, along with Syto 41 to exclude red cell contamination.¹⁰ *Sample was from a mediastinal mass. **There was inadequate sample for Flow MRD but polymerase chain reaction (PCR) MRD was reported as >0.01%. ***Patient had been exposed to 2 days of dexamethasone. UN: unknown; CyTOF: cytometry time of flight; WBC: white blood cell count.

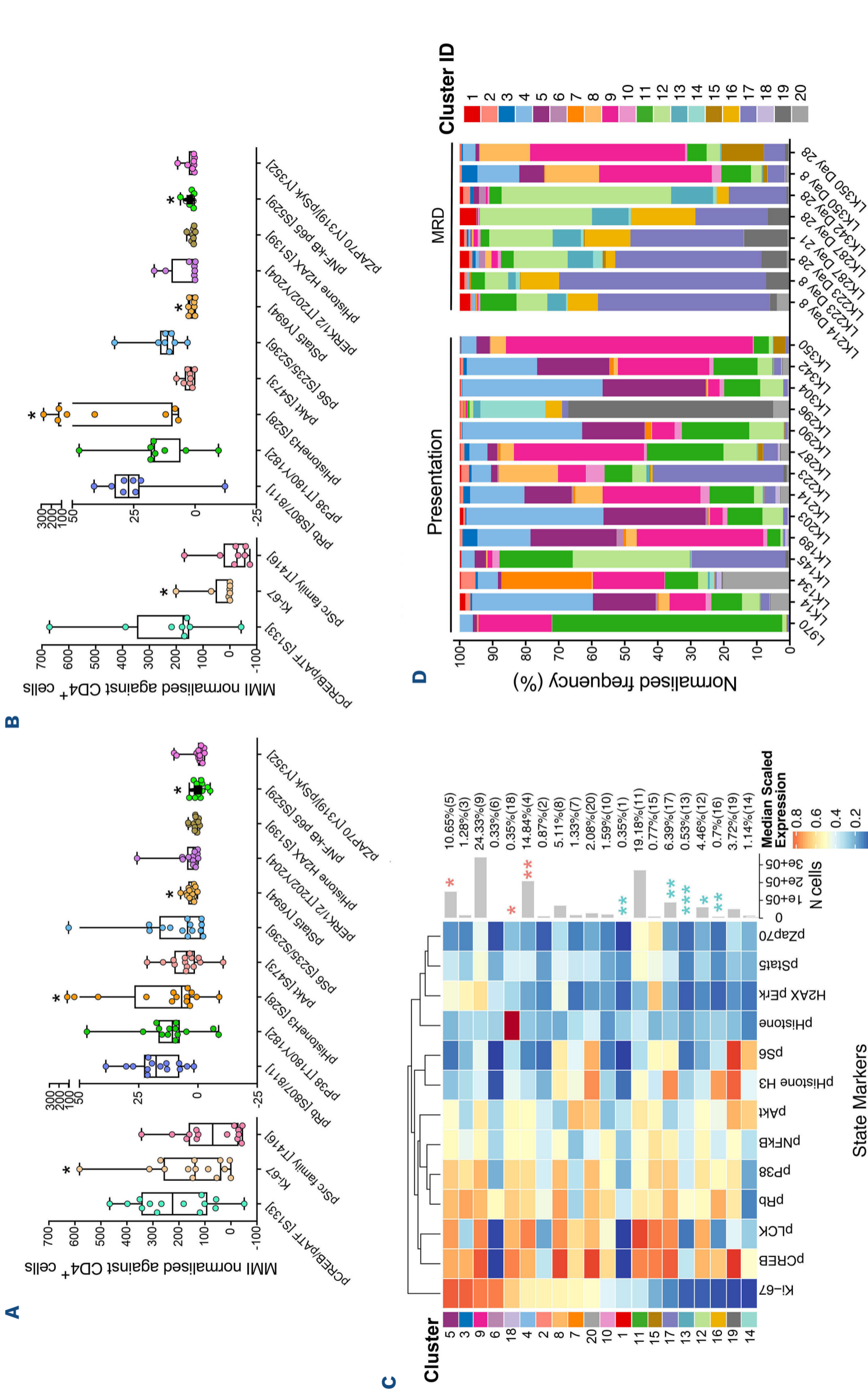


Figure 1. Ubiquitous activation of pCREB in acute lymphoblastic leukemia cell clusters and dormancy of minimal residual disease. Mean mass intensity (MMI) of phospho-markers and Ki67 in presentation T-lineage acute lymphoblastic leukemia (T-ALL) cells (A) and minimal residual disease (MRD) cells (B) normalized against internal CD4⁺ T cells. MMI signals are shown across 2 graphs to better represent data. Heatmap showing median marker expression of 13 phospho-markers across 20 populations generated with FlowSOM after metaclustering with ConsensusClusterPlus using gated ALL cells (C). Heatmap colour shows the median of the arcsinh, 0-1 transformed marker expression calculated from all gated leukemic cells. The column dendrogram shows hierarchical similarity between phospho-markers while the row dendrogram shows the hierarchical similarity between the 20 clusters, generated using the Euclidean distance metric and average linkage. Cluster proportions are shown by barplots and percentages on the right. Asterisks over the barplots denote clusters showing significantly different proportions between Presentation and MRD samples. Pink asterisks are clusters more prominent in Presentation ALL cells and blue asterisks are more prominent in MRD. *Represents values which were considered statistically significant $P < 0.05$, ** for $P < 0.01$ and *** for $P < 0.001$. FlowSOM generated cluster composition by percentage in all patients analysed in study, showing differing trends between presentation and MRD time points (D).

castle Hematology Biobank, after appropriate consent (reference numbers 2002/111 and 07/H0906) from children treated with a with a standard three or four drug induction ALL regimen and who had slow clearance of disease (MRD levels ranging from 0.30% to 56.70% with a mean of 19.99% +/- standard deviation [SD] of 18.50). We analyzed 14 bone marrow samples at presentation of T-ALL and eight samples from five patients during follow-up, taken at day 8 (N=3), day 21 (N=1) and day 28 of induction therapy (N=4) using mass cytometry with previously published methods (antibody panel is shown in *Online Supplementary Table S1*).¹ Patient details are shown in Table 1.

Live, single, non-apoptotic ALL cells were identified by their specific LAIP and the mean mass intensity (MMI) of all antibody signals expressed relative to those from normal CD4-positive cells present in the same sample. The most prominent signals in presentation samples were pCREB/pATF1 [S133] (mean 214.55; range, -50.82 to 466.60), Ki67 (mean 158.97; range, 0.67-582.60) and pSRC family [T416] (mean 80.44; range, -43.90 to 344.16) (Figure 1A; *Online Supplementary Table S2*). The latter having binary separation with high and low activation and likely to reflect levels of pLCK.^{2,3} Western blotting confirmed that the prominent activated form was pCREB, with minimal signal from pATF1 (*Online Supplementary Figure S1*). Compared to presentation ALL cells, MRD cells had a significant decrease in Ki67 levels with a mean of 158.97 falling to 34.62 and an increase in pHH3, with a mean of 21.20 increasing to 87.91 in MRD ($P<0.05$) (Figure 1B; *Online Supplementary Table S2*). There were also more subtle changes in pSTAT5, a signal of 2.96 at presentation decreasing to 1.27 at MRD and an increase in pNFkB p65, -0.30 at presentation increasing to 2.06 in MRD cells ($P<0.05$).

We next used cytometry by time of flight (CyTOF) workflow R pipeline to perform cluster analyses using phospho-signals (and Ki67) from ALL cells to investigate cluster composition in drug naïve cells and in those after therapy. We generated 20 unique ALL cell clusters (Figure 1C, D; *Online Supplementary Table S2*). ALL populations were complex heterogeneous, showing multiple different clusters at both presentation and in MRD cells, but there were clear differences in cluster abundance (Figure 1C). The closely related clusters, 4 and 5, as well as cluster 18, were significantly more represented at presentation ($P<0.05$) and were characterized by multiple signaling nodes including pLCK, pCREB, pRb, pp38 and high Ki67. There were a number of clusters more prevalent in MRD cells including clusters 1, 12, 13, 16 and 17 ($P<0.05$). All of these MRD clusters had strikingly low levels of Ki67, with the more abundant ones also expressing higher levels of pHH3 and pRb. Uniform manifold approximation and projection visualization of MRD and presentation clusters revealed MRD to be enriched in the left and right hand areas of the map. Visualization of pCREB confirmed its almost ubiquitous expression across the UMAP in both presentation

and MRD ALL cells. Clusters 1 and 6 were exceptions in that they expressed low pCREB but represented less than 1% of all cells but cluster 1 was more prominent in MRD (Figures 2A, B and 1C, D). Visualization of Ki67 clearly showed MRD-enriched areas to have significantly lower expression (Figure 2C; *Online Supplementary Figure S3*). This was even more apparent in UMAP projections from individual patients (Figure 2D) and, for patients with multiple time points, there was a further selection of Ki67-negative cells as treatment progressed (LK287, LL223 and LK350). Notably, only one of five patients had MRD cells had both Ki67-negative and positive cell islands (LK360). Clusters 12, 13, 16 and 17 were visible in presentation samples but were clearly more prominent in the MRD (Figure 2E, F).

We next assessed the sensitivity of four patient-derived xenografts (PDX) T-ALL co-cultured with mesenchymal stromal cell support to 666-15, a selective CREB inhibitor, and showed a mean \pm sd, Half maximal inhibitory concentration (IC_{50}) of 3.6 ± 0.2 μ M (Figure 2G). Robust, dose-dependent apoptosis was shown with 666-15 (N=3; $P=0.01$) with almost 100% of cells in the early stages of apoptosis after 48 hours exposure to IC_{50} concentrations (Figure 2H). At the same time point, cell cycle analyses corroborated the cytotoxic action of 666-15 by the increased proportion of cells with subG1 DNA content, though this did not attain statistical significance (N=3; $P=0.07$), and also demonstrated the majority of cells to be in G0/G1 (Figure 2I).

The advancement in cytometric methodologies has provided a stepwise increase in the number of analytic parameters that are enabling extensive functional analyses of rare cell populations, such as clinical MRD. Here, we confirm the presence of activated CREB in almost all T ALL cell clusters at both presentation and MRD and show that MRD is non cycling and, similar to B ALL, is derived from cell populations evident at diagnosis that are enriched during induction therapy. Dormancy is a common mechanism of cancer cells to achieve/acquire multi-drug resistance, at least to therapies reliant upon cell division,⁴ and our data support others in suggesting that ALL MRD cells are dormant.⁵ Eliminating MRD cells at the end of induction might be best achieved with targeted drugs that are not dependent on cycling cells such as the CREB pathway or alternatively re-engaging cell cycling, prior to more standard chemotherapeutics.

CREB overexpression and hyperactivation is reported in a number of cancer types and is considered a therapeutic target as it appears to be a vital signalling node downstream of many oncogenes.⁶ An earlier study by van der Sligte *et al.*, demonstrated that both knockdown and pharmacological inhibition of CREB induced cell cycle arrest and apoptosis in T ALL cells by impacting on genes involved in apoptosis, cell cycle and glucose metabolism.⁷ Here, we confirm the dependency of T-ALL cells on CREB activity with a next generation CREB inhibitor,

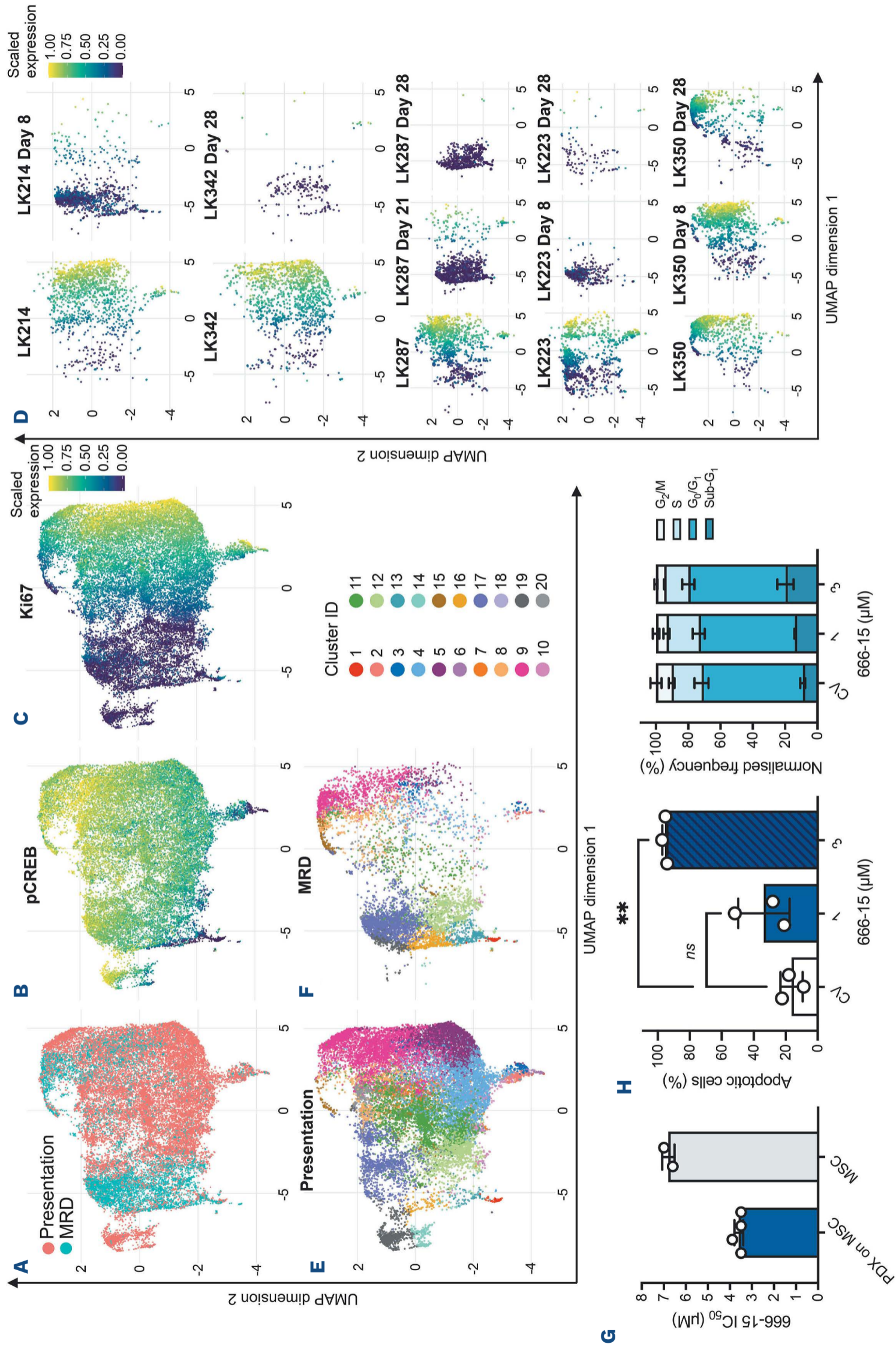


Figure 2. Dormant minimal residual disease cells arise from subpopulations present at diagnosis and the CREB inhibitor 666-15 is cytotoxic in T-cell acute lymphoblastic leukemia cells. Uniform manifold approximation and projection (UMAP) of acute lymphoblastic leukemia (ALL) cells generated using intracellular antibody signals showing cluster segregation in presentation (red) and minimal residual disease (MRD) (blue) samples (A). UMAP of ALL cells showing scaled expression of pCREB (B) and Ki67 (C). UMAP of ALL cells in individual patients showing Ki67 levels in paired presentation and MRD time points (D). UMAP of ALL cells showing cluster distribution in presentation (E) and MRD samples (F). Histogram of 666-15 half maximal inhibitory concentration (IC₅₀) in patient-derived xenografts (PDX) on MSC and MSCs alone (mean ± standard deviation [SD]) are shown (G). Histogram of percentage of apoptotic cells as measured by annexin V binding in cells dosed for 48 hours with control vehicle (CV) or 2 different doses of 666-15 in triplicate PDX (H). Histogram showing the normalized frequency of cells in various stages of the cell cycle in cells dosed for 48 hours with CV or 2 different doses of 666-15 in triplicate PDX. Mean ± SD are shown. **Denotes statistical significance where $P < 0.01$.

666-15. Cytotoxicity was observed at drug concentrations, which reduced tumor growth without overt toxicity in mice models, suggesting a potential therapeutic window of CREB inhibition.^{8,9} Together, these data suggest that MRD-directed therapies should be cell-cycle independent and that the CREB pathway is a valid therapeutic target for both T- and B-lineage ALL cells.

Authors

Dino Masic,¹ Hayden L Bell,¹ Frederik W van Delft,^{1,2} and Julie Anne Elizabeth Irving¹

¹Wolfson Childhood Cancer Research Center, Newcastle University Center for Cancer and ²Department of Pediatric Hematology and Oncology, Great North Children's Hospital, Newcastle upon Tyne, UK

Correspondence:

J. IRVING - Julie.Irving@newcastle.ac.uk

<https://doi.org/10.3324/haematol.2023.284335>

Received: September 26, 2023.

Accepted: February 14, 2024.

Early view: February 22, 2024.

References

1. Masic D, Fee K, Bell H, et al. Hyperactive CREB subpopulations increase during therapy in pediatric B-lineage acute lymphoblastic leukemia. *Haematologica*. 2023;108(4):981-992.
2. Gocho Y, Liu J, Hu J, et al. Network-based systems pharmacology reveals heterogeneity in LCK and BCL2 signaling and therapeutic sensitivity of T-cell acute lymphoblastic leukemia. *Nat Cancer*. 2021;2(3):284-299.
3. Shi Y, Beckett MC, Blair HJ, et al. Phase II-like murine trial identifies synergy between dexamethasone and dasatinib in T-cell acute lymphoblastic leukemia. *Haematologica*. 2021;106(4):1056-1066.
4. Recasens A, Munoz L. Targeting cancer cell dormancy. *Trends Pharmacol Sci*. 2019;40(2):128-141.
5. Ebinger S, Ozdemir EZ, Ziegenhain C, et al. Characterization of rare, dormant, and therapy-resistant cells in acute lymphoblastic leukemia. *Cancer Cell*. 2016;30(6):849-862.
6. Sapio L, Salzillo A, Ragone A, Illiano M, Spina A, Naviglio S. Targeting CREB in cancer therapy: a key candidate or one of many? An update. *Cancers*. 2020;12(11):3166.
7. van der Sligte NE, Kampen KR, ter Elst A, et al. Essential role for cyclic-AMP responsive element binding protein 1 (CREB) in the survival of acute lymphoblastic leukemia. *Oncotarget*. 2015;6(17):14970-14981.
8. Xie F, Li BX, Kassenbrock A, et al. Identification of a potent inhibitor of CREB-mediated gene transcription with efficacious in vivo anticancer activity. *J Med Chem*. 2015;58(12):5075-5087.
9. Li BBX, Gardner R, Xue CH, et al. Systemic Inhibition of CREB is Well-tolerated in vivo. *Sci Rep*. 2016;6:34513.
10. Irving J, Jesson J, Virgo P, et al. Establishment and validation of a standard protocol for the detection of minimal residual disease in B lineage childhood acute lymphoblastic leukemia by flow cytometry in a multi-center setting. *Haematologica*. 2009;94(6):870-874.

©2024 Ferrata Storti Foundation

Published under a CC BY license 

Disclosures

JAEI has received funding from Hoffmann-La Roche Ltd for work unrelated to this manuscript. All other authors have no conflicts of interest to disclose.

Contributions

DM and HLB performed research. JAEI, DM and HLB designed the research study. DM, JAEI, HLB and FWvD analyzed the data. DM and JAEI wrote the first draft of the paper and all authors critically reviewed and approved the final draft.

Acknowledgments

The authors are indebted to Andy Filby and David McDonald from the Newcastle Flow Facility for their expertise in mass cytometric analyses.

Funding

The authors would like to gratefully acknowledge Children with Cancer UK, Newcastle Hospitals NHS Foundation Trust and JGW Paterson for funding this study.

Data-sharing statement

Data is available on request.